

# Dalton Transactions

Accepted Manuscript

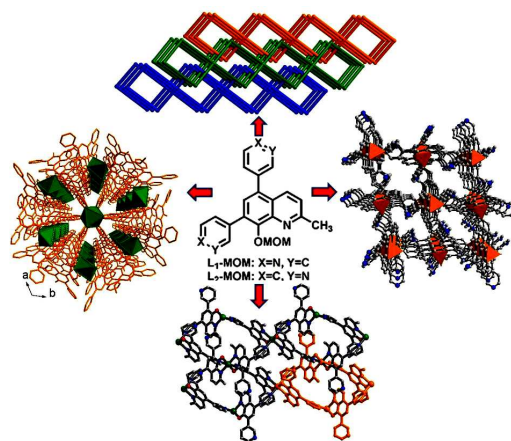


This is an *Accepted Manuscript*, which has been through the Royal Society of Chemistry peer review process and has been accepted for publication.

*Accepted Manuscripts* are published online shortly after acceptance, before technical editing, formatting and proof reading. Using this free service, authors can make their results available to the community, in citable form, before we publish the edited article. We will replace this *Accepted Manuscript* with the edited and formatted *Advance Article* as soon as it is available.

You can find more information about *Accepted Manuscripts* in the [Information for Authors](#).

Please note that technical editing may introduce minor changes to the text and/or graphics, which may alter content. The journal's standard [Terms & Conditions](#) and the [Ethical guidelines](#) still apply. In no event shall the Royal Society of Chemistry be held responsible for any errors or omissions in this *Accepted Manuscript* or any consequences arising from the use of any information it contains.



Five coordination polymers with different structures are prepared under solvothermal conditions. In the solid state, these polymers exhibited disparate fluorescence emission and lifetime due to their different metal centers and supramolecular structures. Interestingly, Fluorescence quenching was also observed when the five coordination polymers were exposed to the vapor of aromatic compounds.

Cite this: DOI: 10.1039/c0xx00000x

www.rsc.org/xxxxxx

ARTICLE TYPE

# Five 8-Hydroxyquinolate-Based Coordination Polymers with Tunable Structures and Photoluminescent Properties for Sensing Nitroaromatics

Liyan Zhang, Liying Sun, Xinyuan Li, Yulan Tian, and Guozan Yuan\*

Received (in XXX, XXX) Xth XXXXXXXXXX 200X, Accepted Xth XXXXXXXXXX 200X

DOI: 10.1039/b000000x

By using two 8-hydroxyquinolate ligands (L<sub>1</sub>-MOM and L<sub>2</sub>-MOM) containing 3-pyridyl or 4-pyridyl group, five novel coordination polymers, namely [Zn<sub>3</sub>(L<sub>1</sub>)<sub>6</sub>] (**1**), [Zn(L<sub>1</sub>)<sub>2</sub>]-2MeOH (**2**), [Zn(L<sub>2</sub>)<sub>2</sub>] (**3**), [Cd(L<sub>2</sub>)<sub>2</sub>] (**4**), and [Cd<sub>4</sub>(L<sub>1</sub>)<sub>6</sub>]-13H<sub>2</sub>O (**5**), were synthesized and characterized by a variety of techniques. Single-crystal X-ray structures have revealed that these coordination polymers exhibit a structural diversification due to the different choices of metal salts and the effect of pyridyl nitrogen position. Compounds **1-5** exhibited different fluorescence emission and lifetime upon excitation in the solid state. The sensing behavior of these polymers was also investigated upon exposure to vapors of various nitroaromatic molecules (analytes). The results show that all five polymers are capable of sensing these nitroaromatic molecules in the vapor phase through fluorescence quenching. Interestingly, **3** exhibits superior sensitivity to the analytes in comparison with other polymers. 2-Nitrotoluene quenches the emission of **3** by as much as 96%.

## Introduction

Coordination polymers (CPs), known as a fascinating organic-inorganic hybrid material class, are certainly very promising as a multifunctional luminescent material because both the inorganic metal cations (or metal clusters) and the organic linkers can provide the platforms to generate luminescence.<sup>1-2</sup> The variety of metal ions, organic ligands, and structural motifs affords an essentially infinite number of combinations.<sup>3</sup> Furthermore, both postsynthetic modification and guest molecules can also emit and/or induce luminescence.<sup>4</sup> These features enable the electronic nature of luminescent CPs to be tailored for a particular application by varying the lumophore type, secondary building units, and their relative spatial arrangements.<sup>5-6</sup> These merits also make them promising candidates for chemical sensing applications.<sup>7</sup> Recently fluorescence active CPs have been applied in the detection of hazardous substances,<sup>8-9</sup> which is an important area of current research for homeland security, environmental safety, and human health. Developing sensitive and efficient explosive detection methods becomes especially urgent in recent years due to the continuing rise of terrorist activities around the globe. In comparison with well-trained canines<sup>10</sup> and sophisticated instrumental methods,<sup>11</sup> optical sensing based on fluorescent materials has the advantages of cost effectiveness and portability.<sup>12</sup> To tailor MOFs for chemical sensing, some CPs with a specific structure and functionality were constructed by the deliberate design and selection of organic linkers and metal-containing units,<sup>13</sup> such as the introduction of guest accessible functional organic groups,<sup>14</sup> and the reservation of open metal sites.<sup>15</sup> The tuned geometry and functionalization of pore may lead to selective adsorption and molecular sensing.<sup>7</sup>

Motivated by the success of tris(8-

hydroxyquinolato)aluminum (Alq<sub>3</sub>) in vacuum-deposited LEDs, the photoluminescent materials based on 8-hydroxyquinoline complexes have in particular attracted a lot of attentions.<sup>16-17</sup> 8-hydroxyquinolate (in its deprotonated form) can bridge the gaps between the neutral bipyridine and the dianionic catecholate because it contains one pyridine donor of bipy and one phenolate unit of catecholate. In addition, the geometry and chelating size of 8-hydroxyquinolate are the same as found for bipy and catecholate, which are very often used as appropriate building blocks for organic ligands. It has been demonstrated that the 8-hydroxyquinoline unit is an ideal building block in metallosupramolecular chemistry.<sup>16-17</sup> With few notable exceptions, 8-hydroxyquinolate-based coordination polymers with desirable structures and functionalities have not yet been developed.<sup>18</sup>

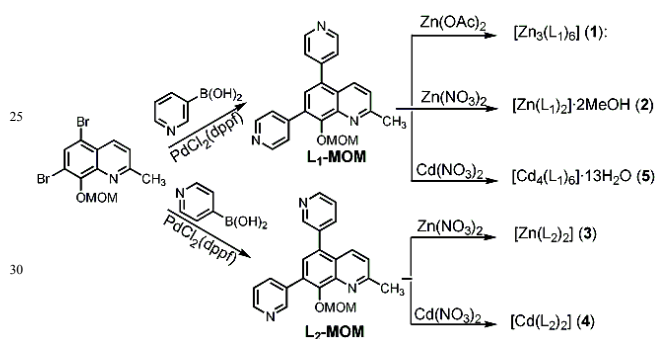
In recent years, our research group has reported a series of photoluminescent complexes involving 2-substituted 8-quinolinolate ligands with NO donor set.<sup>19</sup> Herein, we have synthesized two bispyridyl-based quinoline ligands from the commercial available 8-hydroxyquinoline to form five new Zn(II) and Cd(II) coordination polymers, and characterized the five polymers by a variety of techniques, including microanalysis, IR, and powder and single-crystal X-ray diffraction. The polymeric skeletons exhibit a structural diversification, which can be attributed to the different choices of metal salts and the effect of pyridyl nitrogen position. The investigation of their fluorescent properties shows disparate emission wavelengths and lifetimes in the solid state. In addition, we have also studied the applicability of polymers **1-5** for sensing nitroaromatic molecules at room temperature. The results further suggest that both the electronic properties and supramolecular structures of coordination

polymers may play a key role in the observed fluorescence quenching behavior.

## Results and discussion

### Synthetic Chemistry

The two ligands  $L_1$ -MOM and  $L_2$ -MOM (MOM: methoxymethoxy) were synthesized in more than 90% yield by Suzuki coupling reaction between 3- or 4-pyridylboronic acid and 5,7-dibromo-2-methyl-8-methoxymethoxyquinoline. The  $L_2$ -MOM ligand was fully characterized by  $^1\text{H}$  and  $^{13}\text{C}$  NMR, ESI-MS, and microanalysis. Single crystals of  $[\text{Zn}_3(\text{L}_1)_6]$  (**1**),  $[\text{Zn}(\text{L}_1)_2] \cdot 2\text{MeOH}$  (**2**),  $[\text{Zn}(\text{L}_2)_2]$  (**3**),  $[\text{Cd}(\text{L}_2)_2]$  (**4**), and  $[\text{Cd}_4(\text{L}_1)_6] \cdot 13\text{H}_2\text{O}$  (**5**) were readily obtained in good yield by heating the corresponding Zn(II) or Cd(II) salts and  $L$ -MOM in the mixture of MeOH/DMF/ $\text{H}_2\text{O}$  (scheme 1). It is notable that an anion-dependent self-assembly behavior was observed in **1** and **2**. The  $-\text{MOM}$  group was completely removed from the starting ligands upon reactions with the metal ions. Coordination polymers **1–5** are stable in air and insoluble in water and common organic solvents, and were formulated on the basis of microanalysis, IR, and single-crystal X-ray diffraction



**Scheme 1** Synthesis of ligands  $L_1$ -MOM,  $L_2$ -MOM and polymers **1–5**.

### Structural description

Single crystals of complex **1** was readily obtained in good yields by heating  $\text{Zn}(\text{OAc})_2$  and  $L_1$ -MOM in a mixture of MeOH/DMF. Complex **1** crystallizes in the space group  $P2_1/n$ , with one Zn(II) ion and three  $L_1$  ligands in the asymmetric unit. The MOM groups were completely removed from the starting ligands upon complexation with the metal ions. The Zn1 centre is coordinated by two nitrogen atoms from pyridyl groups, two nitrogen atoms and two oxygen atoms from quinoline rings, forming a  $\text{ZnN}_4\text{O}_2$  slightly distorted octahedral coordination geometry (Fig. 1a). The bond lengths around Zn1 are 2.0338(3) Å for Zn–O, 2.2213(4) Å and 2.2495(4) Å for Zn–N, respectively. The Zn2 centre is five-coordinated by one nitrogen atom of pyridyl group, two oxygen and two nitrogen atoms from two quinoline rings to result in a distorted trigonal bipyramid coordination geometry (Fig. 1a). The distances of Zn–N and Zn–O bonds around Zn2 are 2.0887(4) – 2.2599(3) Å and 1.9336(2) – 1.9612(2) Å, respectively.

In **1**, six  $L_1$  ligands with eight uncoordinated pyridyl groups connect four Zn cations (two Zn1 and two Zn2 atoms) to form a cyclic tetramer  $\text{Zn}_4(\text{L}_1)_6$  (Fig. 1b), which is further linked into a 1D infinite chain along the crystallographic  $a$ -axis. The spacious

nature of one single chain allows another two independent identical chains to penetrate it in a normal mode, thus giving a 3-fold interpenetrated architecture (Fig. 1c and S3). The interdigitation of uncoordinated pyridyl rings from adjacent square grids has efficiently filled all the void space; No any 60 solvent molecules are encapsulated in **1**. Additionally, two

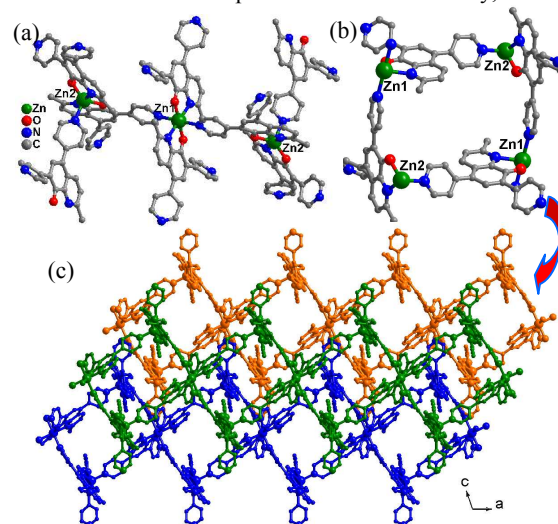


**Fig. 1** (a) Views of the coordination geometries of Zn(II) atoms in **1**; (b) View of a cyclic tetramer  $\text{Zn}_4\text{L}_6$  in **1**; (c) 3-fold interpenetrated architecture in **1**.

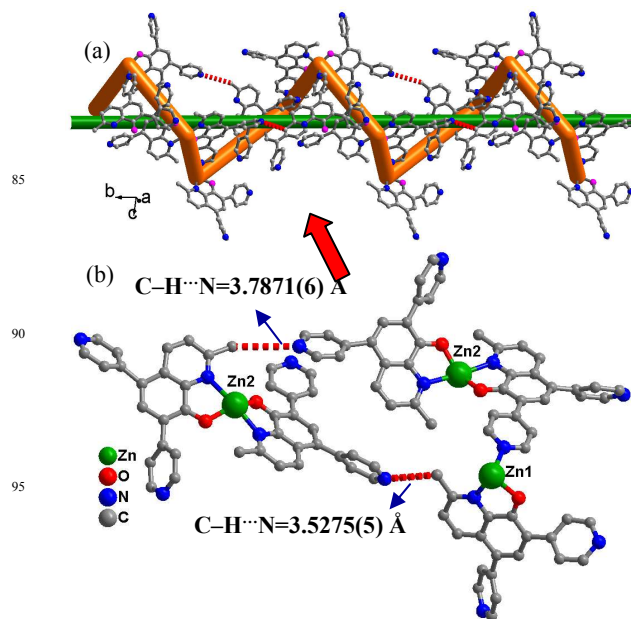


**Fig. 2** (a) View of 1D helical chains fabricated via  $\text{C-H}\cdots\text{N}$  interactions in **1** along the  $b$ -axis; (b) Perspective view of intermolecular  $\text{C-H}\cdots\text{N}$  interactions in **1**.

intertwined helical chains (one is left-handed, the other is right-handed) are constructed via nonclassical  $\text{C-H}\cdots\text{N}$  hydrogen bonds between the C–H group of methyl and the nitrogen atom of pyridine (Fig. 2b,  $\text{C-H}\cdots\text{N}$ : 3.5275(5) Å and 3.7871(6) Å) along the  $b$ -axis with a pitch of 23.6412(43) Å, which is equal to the  $b$  axis length (Fig. 2a). PLATON calculations indicate that complex **1** contains 6.7% void space (341.4 Å<sup>3</sup> per unit cell) that is 110 accessible to solvent molecules.

When  $\text{ZnCl}_2$  was used instead of  $\text{Zn}(\text{NO}_3)_2$  under the same

synthesis condition of **1**, the coordination polymer **2** was obtained as yellow block-like crystals. A single-crystal X-ray diffraction study shows that compound **2** is a 2D network, with one crystallographically independent Zn(II) ion, one L<sub>1</sub> ligand and one uncoordinated CH<sub>3</sub>OH molecule in the asymmetric unit. It crystallizes in the monoclinic system, space group *P*2<sub>1</sub>/*c*. Similar to **1**, the MOM groups were also removed. The metal center Zinc is six-coordinated by two nitrogen atoms from pyridyl groups, two oxygen atoms and two nitrogen atoms from quinoline rings, showing a slightly distorted octahedral coordination geometry (Fig. 3a). The bond lengths around Zn centre are 2.0199(2) Å for Zn-O, 2.2221(2) Å and 2.2428(2) Å for Zn-N, respectively. The Zn(II) metal centers are bridged by L<sub>1</sub> ligands to form a 2D square grid in the *bc* plane (Fig. 3b). It is notable that a kind of *meso*-helical chains (*P+M*) constructed via the metal-ligand coordination interactions are observed in the solid state of this compound (Fig. 4a). These *meso*-helical chains with a pitch of 10.2951(14) Å are alternately arranged along *b* axis, which is identical to the *b* axis length. The 2D layers are further stacked into 3D supramolecular structure (Fig. 4b) via nonclassical C-H...N hydrogen bonds (C-H...N: 3.3489(4) Å) between the C-H group and nitrogen atom from the pyridyl group (Fig. S4). There is significant void space formed between the lamellae, and a space-filling model of **2** viewed along the *a* axis clearly indicates the presence of large channels with a largest dimension of 5.3 Å (Fig. S5). PLATON calculations indicate that complex **2** contains 12.8% void space (222.0 Å<sup>3</sup> per unit cell) that is accessible to solvent molecules.

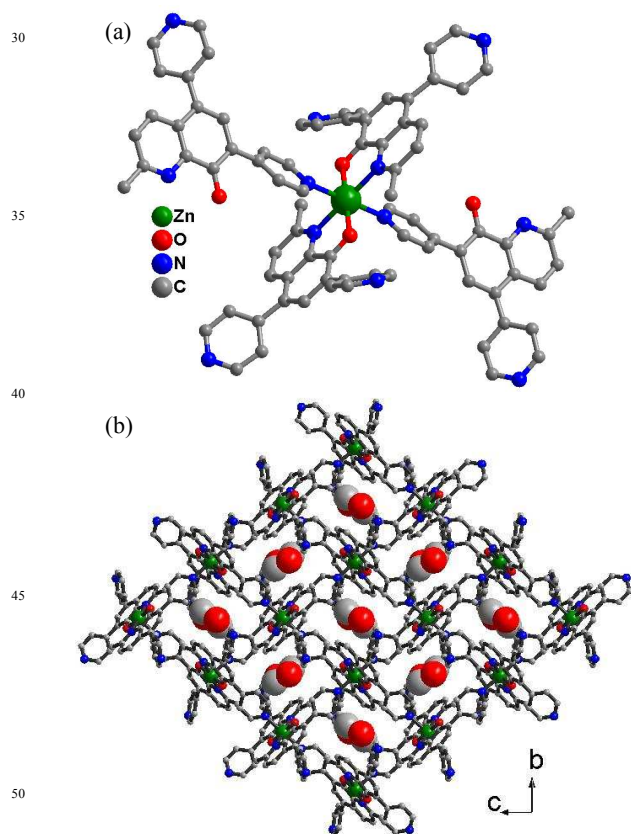


**Fig. 3** (a) View of the coordination geometries of Zn(II) atoms in **2**; (b) 2D square grid of **2** in the *bc* plane (MeOH molecules are indicated by space-filling mode).

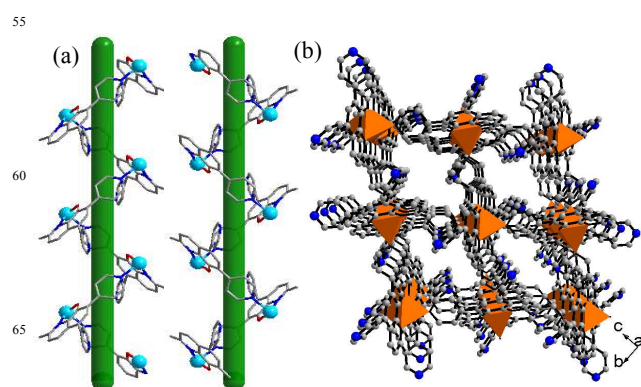


**Fig. 4** (a) The *meso*-helical chains (*P+M*) constructed via the metal-ligand coordination interactions in **2**; (b) View of 3D supramolecular structure in **2**.

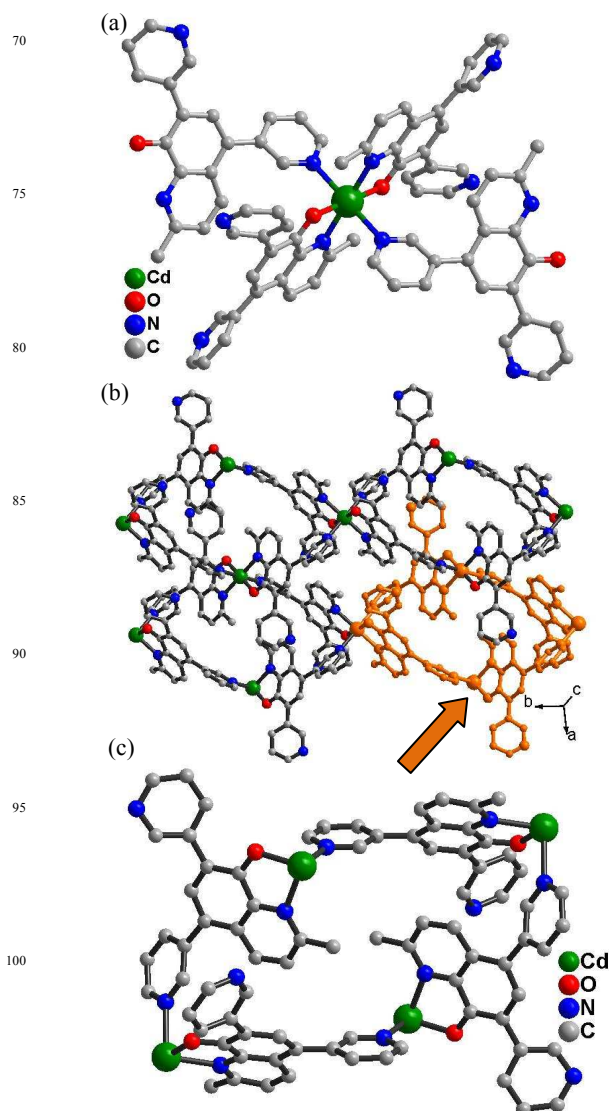


**Fig. 5** (a) View of the coordination geometries of Cd(II) atoms in **4**; (b) 2D square grid of **4** in the *bc* plane.

When the ligand L<sub>2</sub>-MOM reacted with Cd(NO<sub>3</sub>)<sub>2</sub> under the same reaction conditions, the complex **4** was obtained as yellow block-like crystals. Coordination polymer **4** was crystallized in a orthorhombic system and *Pbca* space group. Each asymmetric

unit contains one half of crystallographically distinct Cd(II) ion and one L<sub>2</sub> ligand. The coordination environment of Cd<sup>2+</sup> ions in complex **4** is shown in Fig. 5a, and it can be seen that Cd(II) is six-coordinated to two phenolate oxygen atoms and four nitrogen atoms from four ligands L<sub>2</sub>. The Cd(II) center adopts an octahedral geometry with the equatorial plane occupied by two chelating NO donor sets from two ligands L<sub>2</sub> and the apical position by two pyridyl nitrogen atoms of two other ligands. In the *ab* plane, each Cd atom is linked to four adjacent Cd atoms through the chelating NO donors and pyridyl nitrogen atoms of ligands L<sub>2</sub> to form a 2D grid structure (Fig. 5b). However, no obvious void space for solvent molecules was observed due to the difference of pyridyl nitrogen position compared with that of **2** (Fig. S8). The coordination polymer **3** is isostructural to **4**. The main distinction is that the metal centre was replaced as Zn(II) ion so that there are subtle differences between them.

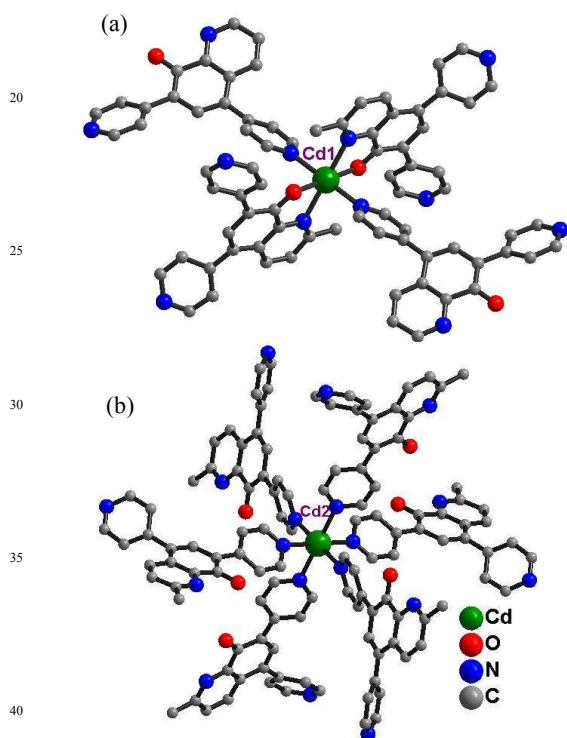


Fig. 6 Views of the coordination geometries of Cd1 (a) and Cd2 (b) in **5**.

X-ray single-crystal diffraction analysis reveals that complex **5** is a 3D network. It crystallizes in the trigonal crystal system with space group of *R*-3. The asymmetric unit contains two crystallographically independent Cd(II) ions. Cd1 is six-coordinated to two nitrogen atoms of pyridyl groups, two oxygen atoms and two nitrogen atoms from quinoline rings, forming a slightly distorted octahedral geometry (Fig. 6a). The bond lengths around Cd1 centre are 2.2104(1) Å for Cd-O, 2.3734(2) Å and 2.3788(1) Å for Cd-N. The Cd2 centre is coordinated to six nitrogen atoms from pyridyl groups, showing an octahedral coordination geometry (Fig. 6b). The bond distance of Cd-N around Cd2 is 2.3849(1) Å. Two Cd1 ions and one Cd2 ion are held together by one L<sub>1</sub> ligand to yield complicated 3D network (Fig. 7b). The most fascinating structural feature of **5** is that six Cd1 centers are arranged around one Cd2 centre to form a chair conformation metallocycle (Fig. 7a). The six Cd1 centers occupy

the edge of the chair, Cd2 centre is in the core of the seat. The distance between Cd1 and Cd2 is 9.1051 Å. One hexagonal channel which is separated to six sections evenly by the pyridyl groups was observed along the *c* axis. PLATON calculations indicate that complex **1** contains 34.5% void space (3420.3 Å<sup>3</sup> per unit cell) that is accessible to solvent molecules.

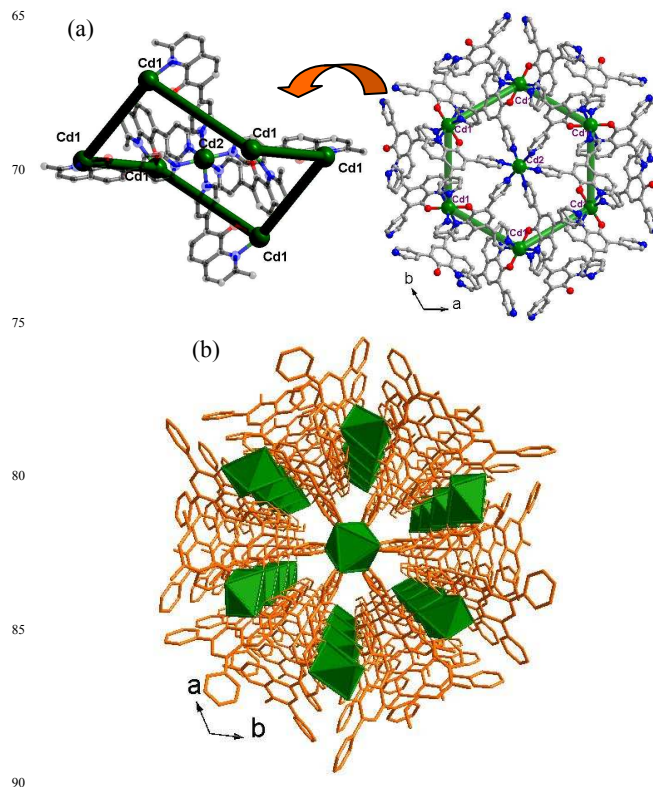


Fig. 7 (a) View of a chair conformation metallocycle fabricated by six Cd1 atoms around one Cd2 centers in **5**; (b) The 3D framework of **5**.

### Photophysical properties

To confirm that the crystal structures of coordination polymers **1-5** are truly representative of their bulk materials tested in photophysical studies, powder X-ray diffraction (PXRD) experiments were carried out on the as-synthesized samples. As we can see from Fig. 8, the peak positions of the experimental and simulated PXRD patterns are in good agreement with each other. The differences in intensity may be owing to the preferred orientation of the crystal samples.

The luminescent behaviors of five complexes and their corresponding free ligands L<sub>1</sub>-MOM and L<sub>2</sub>-MOM were investigated in the solid state at room temperature. When excited with 300 nm light, the free ligands L<sub>1</sub>-MOM and L<sub>2</sub>-MOM display maximum emission wavelengths at 404 and 415 nm, respectively (Fig. 9), which originated from charge transfer of the internal ligand. Coordination polymers **1-5** exhibit intense photoluminescences with the emission maximum at 511, 511, 506, 523, and 543 nm, respectively, upon excitation at 340 nm (Fig. 9). Compared with the emission spectra of the corresponding ligands L<sub>1</sub>-MOM and L<sub>2</sub>-MOM, varying degrees of red shifts of 107 nm in **1** and **2**, 102 nm in **3**, 108 nm in **4**, and 128 nm in **5** have been observed, which are considered to mainly arise from the coordination of metal centers to the ligands L<sub>1</sub>-MOM and L<sub>2</sub>-

MOM. The incorporation of metal ion effectively increases the conformational rigidity of the ligand and reduces the loss of energy via vibration motions<sup>20</sup>. Additionally, the coordination of the ligand with Zn(II) or Cd(II) ions forms additional five-membered rings, which increases the  $\pi$ - $\pi^*$  conjugation length and the conformational coplanarity, accordingly reduces the energy gap between the  $\pi$  and  $\pi^*$  molecular orbital of the ligand<sup>21</sup>. From Fig. 9, the emission wavelengths of polymers **4** and **5** are red-shifted in comparison with those of other three complexes, which may be attributed to their Cd(II) centers and close-packed supramolecular structures.

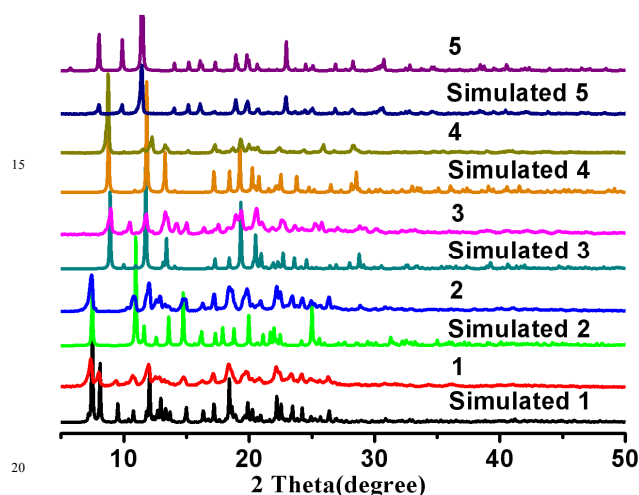


Fig. 8 PXRD patterns of coordination polymers 1-5.

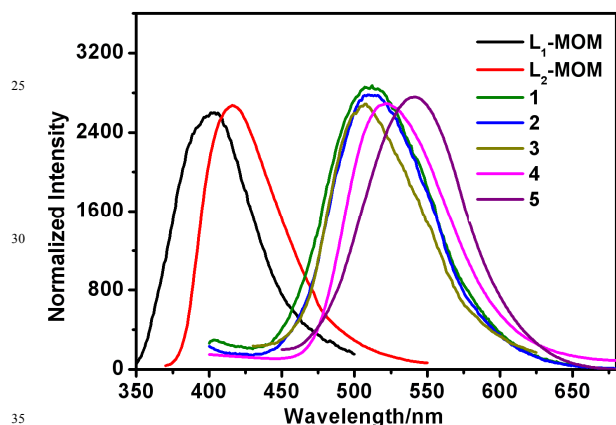


Fig. 9 Emission spectra of ligands L<sub>1</sub>-MOM and L<sub>2</sub>-MOM, coordination polymers 1-5 in the solid state.

To further understand the fluorescent properties of coordination polymers 1-5, their fluorescent lifetimes were investigated at room temperature in the solid state (Fig. S12). The average lifetime was determined by allowing  $\alpha_i$  and  $\tau_i$  to vary, and then convoluting eq 1 with the instrument response function. The data was successfully modeled using double exponentials, and the average lifetime was determined using eq 2. In both equations  $t$  is time,  $\tau$  is lifetime, and  $\alpha$  is a pre-exponential factor<sup>19</sup>. The results are summarized in Table 1. The shortest fluorescence lifetime of coordination polymer **5** (5.75 ns) may arise from a combined contribution from a competitive non-radiative decay process in

the metal complex (such as the incompletely hindered electron transfer), and distinct supramolecular structures in comparison with polymers 1-4.

$$(1) I(t) = \sum_{i=1}^n \alpha_i \exp(-t/\tau_i) \quad (2) \tau_{\text{avg}} = \frac{\alpha_1 \tau_1^2 + \alpha_2 \tau_2^2}{\alpha_1 \tau_1 + \alpha_2 \tau_2}$$

Table 1. Detailed Parameters Extracted from Photoluminescent Properties of 1-5.

| Complex  | $\lambda_{\text{ex}}$ (nm) | $\tau_1$ (ns) | $\tau_2$ (ns) | $\tau_{\text{avg}}$ (ns) |
|----------|----------------------------|---------------|---------------|--------------------------|
| <b>1</b> | 511                        | 4.39(54%)     | 10.53(46%)    | 8.51                     |
| <b>2</b> | 511                        | 5.62(73%)     | 17.43(27%)    | 11.93                    |
| <b>3</b> | 506                        | 5.45(39%)     | 14.32(61%)    | 12.58                    |
| <b>4</b> | 523                        | 3.78(70%)     | 11.42(30%)    | 8.09                     |
| <b>5</b> | 543                        | 3.53(69%)     | 7.94(31%)     | 5.75                     |

$\tau_{\text{avg}}$ : Average fluorescence lifetimes;  $\lambda_{\text{em}}$ : Emission wavelength.

### Sensing of nitroaromatics

Li and coworkers recently explored that many Zn(II) coordination polymers exhibit unique selectivity for the detection of high explosives and other environmentally deleterious aromatics via a fluorescence quenching and enhancement mechanism.<sup>8</sup> This stimulates us to probe the applicability of polymers 1-5 for the sensing of electron-deficient nitroaromatics (NACs). Fluorescent spectra were recorded on powder samples of 1-5 in thin-layer form, and it was found that all nitroaromatics act as fluorescence quenchers for 1-5 (Fig. S13-17). The quenching efficiency (%) was estimated using the formula  $(I_0 - I)/I_0 \times 100\%$ , where  $I_0$  is the maximum fluorescence intensity of the polymers before exposure to the analyte,  $I$  is the maximum intensity after exposure to the analyte. Among these NACs used in this study, the most effective quencher is 2-nitrotoluene (2-NT) compared with nitrobenzene (NB) and 3-nitrotoluene (3-NT) (Fig. 11). 2-NT quenches the emission by 61%, 72%, 96%, 44%, 51%, respectively, for polymer 1-5. For **1**, **2** and **5**, the order of quenching efficiency for the selected nitroaromatics is 2-NT > NB > 3-NT; for **3** and **4**, the quenching efficiency of NACs was found to decrease in the order 2-NT > 3-NT > NB. Notably, this order is not in accordance with the trend of electron-withdrawing groups, which also cannot be explained when the vapor pressure of each analyte is also taken into consideration. The observed fluorescence attenuation can be explained by the donor-acceptor electron-transfer mechanism.<sup>8</sup> 2-NT exhibits the strongest quenching effect may be attributed to its strongest polymer-analyte  $\pi$ -stacking compared with NB and 3-NT<sup>9</sup>. As shown in Fig. 10, the rates of quenching of Zn(II) polymers 1-3 were faster with NACs than that of Cd(II) polymers **4** and **5**. In addition, a higher quenching effect was observed for **3** than isostructural **4** due to their different metal centers. From these data, fluorescence quenching is undergoing a mixed quenching pathway for polymers 1-5. The observed quenching trend is not controlled by a single factor but by a number of properties such as the nature of the analyte molecules, metal centers and supramolecular structures of the coordination polymers, relative orbital energies and interactions between coordination polymers and analyte molecules.<sup>8-9</sup>

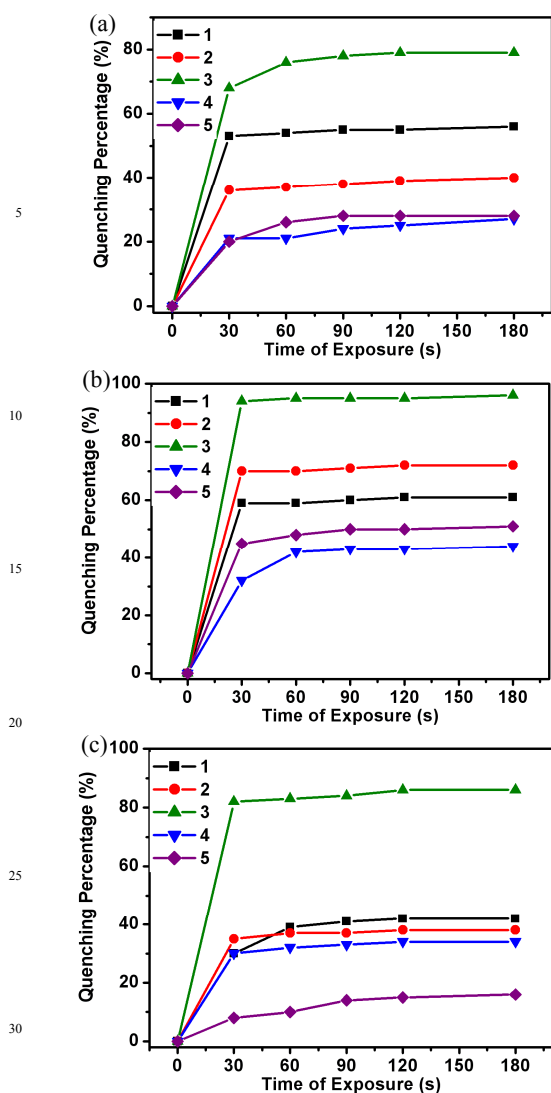


**Fig. 10** Fluorescence quench response of 1-5 upon exposure to saturated vapour of NB (a), 2-NT (b), and 3-NT (c) at room temperature for the specified times.

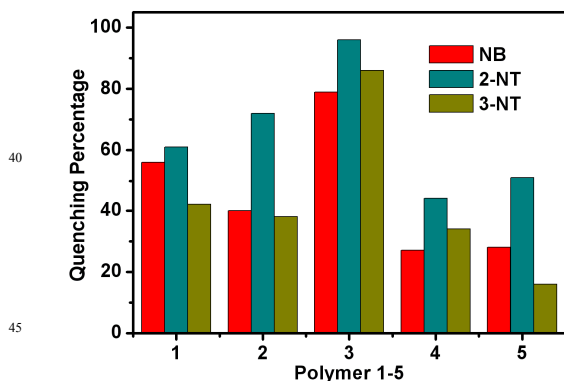


**Fig. 11** Percentage of fluorescence quenching after 3 min by five different analytes for coordination polymers 1-5 at room temperature.

## Experimental Section

### Chemicals, reagents, and analyses

All of the chemicals are commercial available, and used without

further purification. Elemental analyses were performed with an EA1110 CHNS-0 CE elemental analyzer. The IR (KBr pellet) spectrum was recorded (400-4000 $\text{cm}^{-1}$  region) on a Nicolet Magna 750 FT-IR spectrometer. Powder X-ray diffraction (PXRD) data were collected on a DMAX2500 diffractometer using Cu  $K\alpha$  radiation. The calculated PXRD patterns were produced using the SHELXTL-XPOW program and single crystal reflection data. All fluorescence measurements were carried out on a LS 50B Luminescence Spectrometer (Perkin Elmer, Inc., USA). The room-temperature (RT) lifetime measurements were determined on a FLS920 time-resolved and steady-state fluorescence spectrometer (Edinburgh Instruments).  $^1\text{H}$  and  $^{13}\text{C}$  NMR experiments were carried out on a MERCURYplus 400 spectrometer operating at resonance frequencies of 400 MHz. Electrospray ionization mass spectra (ESI-MS) were recorded on a Finnigan LCQ mass spectrometer using dichloromethane-methanol as mobile phase.

### Synthesis

5,7-dibromo-2-methyl-8-methoxymethoxyquinoline and ligand L1-MOM were synthesized according to our previous report.<sup>18b</sup>

Ligand L<sub>2</sub>-MOM: 5,7-dipyridyl-2-methyl-8-methoxymethoxyquinoline (3.6 g, 10.0 mmol), 3-pyridylboronic acid (3.7 g, 30.0 mmol),  $\text{Na}_2\text{CO}_3$  (8.0 g, 75.5 mmol) and  $\text{PdCl}_2(\text{dppf})\cdot\text{CH}_2\text{Cl}_2$  (0.41 g, 0.80 mmol) were weighted into a 100 mL Schlenk flask, which was then pump-purged with  $\text{N}_2$  three times. DME (40 mL) and  $\text{H}_2\text{O}$  (20 mL) were added under a dry  $\text{N}_2$  atmosphere. The mixture was stirred at 95  $^\circ\text{C}$  for overnight. The reaction mixture was cooled to room temperature and extracted with  $\text{CH}_2\text{Cl}_2$ . The organic layers were dried over anhydrous  $\text{Na}_2\text{SO}_4$  and then concentrated under reduced pressure. The crude product was purified by column chromatography on silica gel (8:3:1 AcOEt-hexane- $\text{Et}_3\text{N}$ ) to afford ligand L<sub>2</sub>-MOM as a white solid. Yield: 3.0, 84%.  $^1\text{H}$  NMR (400 MHz,  $\text{CDCl}_3$ )  $\delta$ : 8.96 (d,  $J = 2$  Hz, 1H), 8.74 (d,  $J = 2$  Hz, 1H), 8.69 (dd,  $J = 6.4$  Hz, 1H), 8.61 (dd,  $J = 6.4$  Hz, 1H), 8.06-8.01 (m, 2H), 7.80-7.77 (m, 1H), 7.46-7.39 (m, 3H), 7.29 (d,  $J = 8.8$  Hz, 1H), 5.43 (s, 2H), 3.03 (s, 3H), 2.76 (s, 3H).  $^{13}\text{C}$  NMR(400 MHz,  $\text{CDCl}_3$ )  $\delta$ : 159.2, 150.9, 150.7, 150.1, 149.2, 148.7, 142.6, 137.5, 135.0, 134.3, 132.6, 131.0, 128.6, 126.3, 123.6, 123.3, 123.0, 100.4, 57.5, 25.8; ESI-MS:  $m/z$  358.1( $[\text{M}+1]^+$ ), 359.0( $[\text{M}+2]^+$ ). Elemental analysis (%): calcd for ( $\text{C}_{22}\text{H}_{19}\text{N}_3\text{O}_2$ ) C: 73.93, H: 5.36, N: 11.76; found C: 73.75, H: 5.27, N: 11.88.

Synthesis of compounds 1-5: A mixture of  $\text{ZnX}_2$  ( $\text{X} = \text{OAc}^-$ ,  $\text{NO}_3^-$ , 0.08 mmol) or  $\text{Cd}(\text{NO}_3)_2$  (0.08 mmol), L<sub>1</sub>-MOM or L<sub>2</sub>-MOM (0.04 mmol),  $\text{H}_2\text{O}$  (0.2 mL), DMF (0.2 mL) and MeOH (2 mL) in a capped vial was heated at 80  $^\circ\text{C}$  for one day. Yellow blocklike crystals of 1-5 suitable for single-crystal X-ray diffraction were collected, washed with ether and dried in air. Yield: 1, 11.3 mg, 82%; 2, 12.1 mg, 80%; 3, 11.5 mg, 85%; 4, 11.6 mg, 79%; 5, 13.6 mg, 80%

Compound 1: 1 was prepared by solvothermal reactions of  $\text{Zn}(\text{OAc})_2$  with ligand L<sub>1</sub>-MOM according to above general procedure. Elemental Analysis data and IR of  $[\text{Zn}_3(\text{L}_1)_6]$  (1): Anal (%). Calcd for  $\text{C}_{120}\text{H}_{84}\text{N}_{18}\text{O}_6\text{Zn}_3$ : C, 69.62; H, 4.09; N, 12.18. Found: C, 69.13; H, 4.16; N, 12.03. FTIR (KBr pellet): 3748(w), 3449(s), 3425(s), 1598(s), 1548(w), 1514(w), 1419(s), 1363(w), 1271(m), 1224(w), 1104(w), 1065(w), 1020(w), 834(m), 750(m),



656(w), 580(m), 557(w), 509(w).

Compound **2**: **2** was prepared by solvothermal reactions of Zn(NO<sub>3</sub>)<sub>2</sub> with ligand L<sub>1</sub>-MOM according to above general procedure. Elemental Analysis data and IR of [Zn(L<sub>1</sub>)<sub>2</sub>] $\cdot$ 2MeOH (**2**): Anal (%). Calcd for C<sub>42</sub>H<sub>36</sub>N<sub>6</sub>O<sub>4</sub>Zn: C, 66.89; H, 4.81; N, 11.14. Found: C, 66.65; H, 4.90; N, 11.34. FTIR (KBr pellet): 3446(s), 3025(w), 1598(s), 1548(m), 1513(m), 1435(s), 1409(s), 1364(m), 1318(w), 1272(m), 1216(w), 1104(w), 1065(w), 1017(w), 832(m), 749(w), 695(w), 684(w), 656(w), 584(m), 522(w).

Compound **3**: **3** was prepared by solvothermal reactions of Zn(NO<sub>3</sub>)<sub>2</sub> with ligand L<sub>2</sub>-MOM according to above general procedure. Elemental Analysis data and IR of [Zn(L<sub>2</sub>)<sub>2</sub>] (**3**): Anal (%). Calcd for C<sub>40</sub>H<sub>28</sub>N<sub>6</sub>O<sub>2</sub>Zn: C, 69.62; H, 4.09; N, 12.18. Found: C, 69.46; H, 4.36; N, 12.01. FTIR (KBr pellet): 3867(w), 3785(w), 3449(s), 3058(w), 1624(w), 1516(m), 1420(s), 1364(m), 1326(w), 1272(m), 1186(m), 1107(m), 1029(w), 950(w), 901(w), 823(m), 754(m), 710(m), 655(w), 630(w), 578(w).

Compound **4**: **4** was prepared by solvothermal reactions of Cd(NO<sub>3</sub>)<sub>2</sub> with ligand L<sub>2</sub>-MOM according to above general procedure. Elemental Analysis data and IR of [Cd(L<sub>2</sub>)<sub>2</sub>] (**4**): Anal (%). Calcd for C<sub>40</sub>H<sub>28</sub>N<sub>6</sub>O<sub>2</sub>Cd: C, 65.18; H, 3.83; N, 11.40. Found: C, 65.02; H, 3.98; N, 11.24. FTIR (KBr pellet): 3423(w), 3273(w), 3082(w), 2854(w), 2805(w), 2575(w), 2160(w), 1888(m), 1752(m), 1674(m), 1566(m), 1520(m), 1427(s), 1357(s), 1263(m), 1179(w), 1143(w), 1101(w), 1049(m), 974(w), 948(s), 897(w), 801(w), 750(w), 707(w), 628(w), 566(w), 538(s).

Compound **5**: **5** was prepared by solvothermal reactions of Cd(NO<sub>3</sub>)<sub>2</sub> with ligand L<sub>1</sub>-MOM according to above general procedure. Elemental Analysis data and IR of [Cd<sub>4</sub>(L<sub>1</sub>)<sub>6</sub>] $\cdot$ 13H<sub>2</sub>O (**5**): Anal (%). Calcd for C<sub>120</sub>H<sub>110</sub>N<sub>18</sub>O<sub>19</sub>Cd<sub>4</sub>: C, 56.35; H, 4.33; N, 9.86. Found: C, 56.77; H, 4.28; N, 9.95. FTIR (KBr pellet): 3750(m), 3673(m), 3540(m), 3463(m), 3419(m), 3261(w), 3189(w), 2834(w), 2805(w), 2595(w), 2563(w), 1885(w), 1841(w), 1748(w), 1655(m), 1604(s), 1547(m), 1514(m), 1385(s), 1260(w), 1216(w), 1171(w), 1062(m), 1006(m), 949(m), 832(m), 740(w), 655(m), 581(m).

#### Preparation of thin layers for photoluminescence study

For photoluminescence (PL) studies, samples were prepared in the form of thin layers on glass slides. Quartz slides of dimension 1 $\times$ 2 cm were first rinsed with de-ionized water and methanol, and then dried in the oven. Double sided tape was then applied to the upper half of the slide. For making the thin layers of the sample, the tape was peeled off from the slide after 5 minutes, so that the glue from the tape is stuck in the glass slide. well-ground powder of the as-made sample was then sprinkled evenly onto the glued surface of the slide. The extra samples were removed by gentle tapping and putting the face of the slide down. By this process a very thin continuous layer of sample was formed on the glass surface. This glass was then used for the PL study of the sample. New slides with a thin layer were used for each of the quenching experiment. The original fluorescence spectra of each layer were collected before placing the particular glass slides onto each of the vapors of NACs was ascertained by inserting the prepared thin layers into quartz cuvette at RT containing the analytes and cotton gauze, which prevents the direct contact of the thin layers with the analyte and helps to maintain a constant saturated vapor

pressure. Thin layers were placed in the quartz cuvette and fluorescence spectra were measured after exposing the thin layers for a specific interval time.

#### X-ray crystallography

Single-crystal XRD data for compounds **1-5** were all collected on a Bruker APEX area-detector X-ray diffractometer with MoK $\alpha$  radiation ( $\lambda = 0.71073$  Å). The empirical absorption correction was applied by using the SADABS program (G. M. Sheldrick, SADABS, program for empirical absorption correction of area detector data; University of Göttingen, Göttingen, Germany, 1996). The structure was solved using direct method, and refined by full-matrix least-squares on  $F^2$  (G. M. Sheldrick, SHELXTL97, program for crystal structure refinement, University of Göttingen, Germany, 1997). In coordination polymers **1** and **5**, the solvent-masking procedure (aka SQUEEZE) has been applied to the entire contents of the voids. Crystal data and details of the data collection are given in Table S1, whereas the selected bond distances and angles are presented in Table S2-6. The CCDC numbers of **1-5** are 1016361-1016365, respectively.

#### Conclusion

In summary, five coordination polymers with different structures are prepared under solvothermal conditions, using Zn(II) or Cd(II) salts and two bispyridyl-based quinolate ligands synthesized from the cheap commercial available 8-hydroxyquinaldine. These polymers exhibited disparate fluorescence emission and lifetime upon excitation in the solid state due to their different metal centers and supramolecular structures. We have also evaluated the fluorescence-based sensing properties of **1-5** at room temperature. Fluorescence quenching was observed when the coordination polymers were exposed to the vapor of aromatic compounds. However, compound **3** shows superior sensitivity to the analytes in comparison with other polymers. The rate of quenching of polymers **1-5** was higher with 2-NT compared to those with NB and 3-NT. This work shows that fluorescence quenching is undergoing a mixed quenching pathway, and governed by a number of factors such as the nature of the analyte molecules, metal centers and supramolecular structures of the coordination polymers, relative orbital energies and interactions between coordination polymers and analyte molecules.

#### Acknowledgements

This work was supported by the National Natural Science Foundation of China (Nos. 21201002), and Anhui Provincial Natural Science Foundation (1308085QB22). Provincial natural science research program of higher education institutions of Anhui Province (KJ2013Z028). National Training Programs of Innovation and Entrepreneurship for Undergraduates (201310360028). Training Programs of Innovation and Entrepreneurship of Anhui Province for Undergraduates (AH201310360152).

#### Notes and references

L. Zhang, L. Sun, X. Li, Y. Tian, Prof. Dr. G. Yuan  
School of Chemistry and Chemical Engineering  
Anhui University of Technology

Maanshan 243002 (P. R. China)

Fax: (+86)555 2311552

E-mail: yuanguozan@163.com

Supporting information for this article is given via a link at the end of the document. (Please delete this text if not appropriate)

- 1 (a) M. Suh, Y. Cheon, E. Lee, *Coord. Chem. Rev.*, 2008, **252**, 1007-1026; (b) D. Maspoch, D. Ruiz-Molina, J. Veciana, *Chem. Soc. Rev.*, 2007, **36**, 770-818; (c) J. Rocha, L. D. Carlos, F. A. A. Paz, D. Ananias, *Chem. Soc. Rev.*, 2011, **40**, 926-940; (d) M. D. Allendorf, C. A. Bauer, R. K. Bhakta, R. J. T. Houk, *Chem. Soc. Rev.*, 2009, **38**, 1330-1352; (e) B. Chen, S. Xiang, G. Qian, *Acc. Chem. Res.*, 2010, **43**, 1115; (f) O. Shekha, J. Liu, R. A. Fischer, C. Wöll, *Chem. Soc. Rev.*, 2011, **40**, 1081-1106; (g) G. Férey, *Chem. Soc. Rev.*, 2008, **37**, 191-214; (h) Y. Cui, Y. Yue, G. Qian, B. Chen, *Chem. Rev.*, 2012, **112**, 1126-1162.
- 2 (a) X. Yang, R. A. Jones, S. Huang, *Coord. Chem. Rev.*, 2014, **273**, 63-75; (b) Y. Cui, B. Chen, G. Qian, *Coord. Chem. Rev.*, 2014, **273**, 76-86; (c) Y. Zhou, X. Li, L. Zhang, Y. Guo, Z. Shi, *Inorg. Chem.*, 2014, **53**, 3362-3370; (d) J. -S. Qin, S. -J. Bao, P. Li, W. Xie, D. -Y. Du, L. Zhao, Y. -Q. Lan, Z. -M. Su, *Chem. Asian J.*, 2014, **9**, 749-753.
- 3 (a) K. Mo, Y. Yang, Y. Cui, *J. Am. Chem. Soc.*, 2014, **136**, 1746-1749; (b) W. Xuan, C. Zhu, Y. Liu, Y. Cui, *Chem. Soc. Rev.*, 2012, **41**, 1677-1695; (c) Y. Liu, W. Xuan, Y. Cui, *Adv. Mater.*, 2010, **22**, 4112-4135; (d) X. Xi, Y. Fang, T. Dong, Y. Cui, *Angew. Chem. Int. Ed.*, 2011, **50**, 1154-1158; (e) Y. Liu, X. Xu, F. Zheng, Y. Cui, *Angew. Chem. Int. Ed.*, 2008, **47**, 4538-4541. (f) Y. He, B. Li, M. O'Keefe, B. Chen, *Chem. Soc. Rev.*, 2014, **43**, 5618-5656; (g) Y. -F. Han, W. -G. Jia, W. -B. Yu, G. -X. Jin, *Chem. Soc. Rev.*, 2009, 3419-3434; (h) Y. -F. Han, W. -G. Jia, Y. -J. Lin, G. -X. Jin, *Angew. Chem. Int. Ed.*, 2009, **48**, 6234-6238; (i) Y. -F. Han, H. Li, G. -X. Jin, *Chem. Commun.*, 2010, **46**, 6879-6890; (j) S. -L. Huang, Y. -J. Lin, T. S. A. Hor, G. -X. Jin, *J. Am. Chem. Soc.*, 2013, **135**, 8125-8128; (k) Z. -J. Yao, W. -B. Yu, Y. -J. Lin, S. -L. Huang, Z. -H. Li, G. -X. Jin, *J. Am. Chem. Soc.*, 2014, **136**, 2825-2832; (l) H. Li, Y. -F. Han, Y. -J. Lin, Z. -W. Guo, G. -X. Jin, *J. Am. Chem. Soc.*, 2014, **136**, 2982-2985.
- 4 (a) J. An, C. M. Shade, D. A. Chengelis-Czegan, S. P. Petoud, N. L. Rosi, *J. Am. Chem. Soc.*, 2011, **133**, 1220-1223; (b) F. Luo, S. R. Batten, *Dalton Trans.*, 2010, **39**, 4485-4488; (c) Q. R. Fang, G. S. Zhu, Z. Jin, Y. Y. Ji, J. W. Ye, M. Xue, H. Yang, Y. Wang, S. L. Qiu, *Angew. Chem. Int. Ed.*, 2007, **46**, 6638-6642; (d) S. Jung, Y. Kim, S. J. Kim, T. H. Kwon, S. Huh, S. Park, *Chem. Commun.*, 2011, **47**, 2904-2906.
- 5 (a) L. Wen, Y. Li, Z. Lu, J. Lin, C. D. Meng, *Cryst. Growth Des.*, 2006, **6**, 530-537; (b) X. L. Wang, Q. Chao, E. B. Wang, X. Lin, Z. M. Su, C. W. Hu, *Angew. Chem. Int. Ed.*, 2004, **43**, 5036-5040; (c) C. A. Bauer, T. V. Timofeeva, T. B. Settersten, B. D. Patterson, V. H. Liu, B. A. Simmons, M. D. Allendorf, *J. Am. Chem. Soc.*, 2007, **129**, 7136-7144; (d) Z. F. Chen, R. G. Xiong, J. Zhang, X. T. Chen, Z. L. Xue, X. Z. You, *Inorg. Chem.*, 2001, **40**, 4075-4077; (e) H. C. Wu, P. Thanasekaran, C. H. Tsai, J. Y. Wu, S. M. Huang, Y. S. Wen, K. L. Lu, *Inorg. Chem.*, 2006, **45**, 295-303; (f) N. B. Shustova, A. F. Cozzolino, M. Dincă, *J. Am. Chem. Soc.*, 2012, **134**, 19596-19599.
- 6 (a) A. Stein, S. W. Keller, T. E. Mallouk, *Science*, 1993, **259**, 1558-1564; (b) M. Eddaoudi, J. Kim, N. Rosi, D. Vodak, J. Wachter, M. O'Keefe, O. M. Yaghi, *Science*, 2002, **295**, 469-472; (c) B. L. Chen, C. D. Liang, J. Yang, D. S. Contreras, Y. L. Clancy, E. B. Lobkovsky, O. M. Yaghi, S. Dai, *Angew. Chem. Int. Ed.*, 2006, **45**, 1390-1393; (d) T. Li, J. Yang, X. J. Hong, Y. J. Ou, Z. G. Gu, Y. P. Cai, *CrystEngComm*, 2014, **16**, 3848-3852; (e) T. Li, X. J. Hong, X. Liu, R. Chen, Q. G. Zhan, X. Xu, Y. P. Cai, *CrystEngComm*, 2014, **16**, 3883-3889; (f) Z. G. Gu, Y. T. Liu, X. J. Hong, Q. G. Zhan, Z. P. Zheng, S. R. Zheng, W. S. Li, S. J. Hu, Y. P. Cai, *Cryst. Growth Des.*, 2012, **12**, 2178-2186.
- 7 (a) L. E. Kreno, K. Leong, O. K. Farha, M. Allendorf, R. P. V. Duyne, J. T. Hupp, *Chem. Rev.*, 2012, **112**, 1105-1125; (b) L. J. Murray, M. Dinca, J. R. Long, *Chem. Soc. Rev.*, 2009, **38**, 1294-1314.
- 8 (a) Z. Hu, B. J. Deibert, J. Li, *Chem. Soc. Rev.*, 2014, **43**, 5815-5840; (b) A. Lan, K. Li, H. Wu, D. H. Olson, T. J. Emge, W. Ki, M. Hong, J. Li, *Angew. Chem. Int. Ed.*, 2009, **48**, 2334-2338; (c) A. Lan, K. Li, H. Wu, L. Kong, N. Nijem, D. H. Olson, T. J. Emge, Y. J. Chabal, D. C. Langreth, M. Hong, J. Li, *Inorg. Chem.*, 2009, **48**, 7165-7173; (d) S. Pramanik, C. Zheng, X. Zhang, T. J. Emge, J. Li, *J. Am. Chem. Soc.*, 2011, **133**, 4153-4155; (e) S. Pramanik, Z. Hu, X. Zhang, C. Zheng, S. Kelly, J. Li, *Chem. Eur. J.*, 2013, **19**, 15964-15971; (f) D. Banerjee, Z. Hu, S. Pramanik, X. Zhang, H. Wang, J. Li, *CrystEngComm*, 2013, **15**, 9745-9750.
- 9 (a) B. Gole, A. K. Bar, P. S. Mukherjee, *Chem. Eur. J.*, 2014, **20**, 2276-2291; (b) G. Liu, Y. Qin, L. Jing, G. Wei, H. Li, *Chem. Commun.*, 2013, **49**, 1699-1701; (c) Y. S. Xue, Y. He, L. Zhou, F. J. Chen, Y. Xu, H. B. Du, X. Z. You, B. Chen, *J. Mater. Chem.*, 2013, **1**, 4525-4530; (d) T. K. Kim, J. H. Lee, D. Moon, H. R. Moon, *Inorg. Chem.*, 2013, **52**, 589-595; (e) C. Zhu, W. Xuan, Y. Cui, *Dalton Trans.*, 2012, **41**, 3928-3932.
- 10 K. G. Furton, L. J. Myers, *Talanta*, 2001, **54**, 487-500.
- 11 (a) K. Håkansson, R. V. Coorey, R. A. Zubarev, V. L. Talrose, P. Håkansson, *J. Mass Spectrom.*, 2000, **35**, 337-346; (b) J. M. Sylvia, J. A. Janni, J. D. Klein, K. M. Spencer, *Anal. Chem.*, 2000, **72**, 5834-5840; (c) S. F. Hollowell, *Talanta*, 2001, **54**, 447-458; (d) R. D. Luggar, M. J. Farquharson, J. A. Horrocks, R. J. Lacey, *X-Ray Spectrom.*, 1998, **27**, 87-94.
- 12 Y. Salinas, R. Martinez-Manez, M. D. Marcos, F. Sancenon, A. M. Costero, M. Parra, S. Gil, *Chem. Soc. Rev.*, 2012, **41**, 1261-1296.
- 13 (a) S. D. Burd, S. Q. Ma, J. A. Perman, B. J. Sikora, R. Q. Snurr, P. K. Thallapally, J. Tian, L. Wojtas, M. J. Zaworotko, *J. Am. Chem. Soc.*, 2012, **134**, 3663-3666; (b) S. T. Zheng, T. Wu, C. Chou, A. Fuhr, P. Y. Feng, X. H. Bu, *J. Am. Chem. Soc.*, 2012, **134**, 4517-4520; (c) T. M. McDonald, W. R. Lee, J. A. Mason, B. M. Wiers, C. S. Hong, J. R. Long, *J. Am. Chem. Soc.*, 2012, **134**, 7056-7065; (d) V. Colombo, C. Montoro, A. Maspero, G. Palmisano, N. Masciocchi, S. Galli, E. Barea, J. A. R. Navarro, *J. Am. Chem. Soc.*, 2012, **134**, 12830-12843.
- 14 (a) A. R. Millward, O. M. Yaghi, *J. Am. Chem. Soc.*, 2005, **127**, 17998-17999; (b) B. Wang, A. P. Côté, H. Furukawa, M. O'Keefe, O. M. Yaghi, *Nature*, 2008, **453**, 207-211; (c) R. K. Deshpande, J. L. Minnaar, S. G. Telfer, *Angew. Chem. Int. Ed.*, 2010, **49**, 4598-4602.
- 15 (a) R. Kitaura, G. Onoyama, H. Sakamoto, R. Matsuda, S. Noro, S. Kitagawa, *Angew. Chem. Int. Ed.*, 2004, **43**, 2684-2687; (b) S. C. Xiang, W. Zhou, Z. J. Zhang, M. A. Green, Y. Liu, B. Chen, *Angew. Chem., Int. Ed.*, 2010, **49**, 4615-4618; (c) H. Deng, S. Grunder, K. E. Cordova, C. Valente, H. Furukawa, M. Hmadeh, F. Gándara, A. C. Whalley, Z. Liu, S. Asahina, H. Kazumori, M. O'Keefe, O. Terasaki, J. F. Stoddart, O. M. Yaghi, *Science*, 2012, **336**, 1018-1023.
- 16 (a) M. Albrecht, M. Fiege, O. Osetska, *Coord. Chem. Rev.*, 2008, **252**, 812-824; (b) K. Sokolowski, I. Justyniak, W. Śliwiński, K. Sołtys, A. Tulewicz, A. Kornowicz, R. Moszyński, J. Lipkowski, J. Lewiński, *Chem. Eur. J.*, 2012, **18**, 5637-5645; (c) K. Sokolowski, W. Bury, I. Justyniak, D. Fairen-Jimenez, K. Sołtys, D. Prochowicz, S. Yang, M. Schröder, J. Lewiński, *Angew. Chem. Int. Ed.*, 2013, **52**, 13414-13418; (d) D. Prochowicz, K. Sokolowski, J. Lewiński, *Coord. Chem. Rev.*, 2014, **270-271**, 112-126.
- 17 (a) C. W. Tang, S. A. VanSlyke, *Appl. Phys. Lett.*, 1987, **51**, 913-915; (b) M. Brinkmann, G. Gadret, M. Muccini, C. Taliani, N. Masciocchi, A. Sironi, *J. Am. Chem. Soc.*, 2000, **122**, 5147-5157; (c) M. Cöle, R. E. Dinnebier, W. Brütting, *Chem. Commun.*, 2002, 2908-2909; (d) H. Bi, H. Zhang, Y. Zhang, H. Gao, Z. Su, Y. Wang, *Adv. Mater.*, 2010, **22**, 1631-1634.
- 18 (a) F. Du, H. Wang, Y. Bao, B. Liu, H. Zheng, R. Bai, *J. Mater. Chem.*, 2011, **21**, 10859-10864; (b) G. Yuan, W. Shan, B. Liu, L. Rong, L. Zhang, H. Zhang, X. Wei, *Dalton Trans.*, 2014, **43**, 9777-9785.
- 19 (a) G. Yuan, Y. Huo, X. Nie, X. Fang, S. Zhu, *Tetrahedron*, 2012, **68**, 8018-8023; (b) G. Yuan, Y. Huo, L. Rong, X. Nie, X. Fang, *Inorg. Chem. Commun.*, 2012, **23**, 90-94; (c) G. Yuan, Y. Huo, X. Nie, H. Jiang, B. Liu, X. Fang, F. Zhao, *Dalton Trans.*, 2013, **42**, 2921-2929; (d) G. Yuan, L. Rong, X. Qiao, L. Ma, X. Wei, *CrystEngComm*, 2013, **15**, 7307-7314; (e) G. Yuan, W. Shan, X. Qiao, L. Ma, Y. Huo, *Chem. Asian J.*, 2014, **9**, 1913-1921.
- 20 (a) M. D. Zhang, L. Qin, H. T. Yang, Y. Z. Li, Z. J. Guo, H. G. Zheng, *Cryst. Growth Des.*, 2013, **13**, 1961-1969; (b) X. X. Zhou, H. C. Fang, Y. Y. Ge, Z. Y. Zhou, Z. G. Gu, X. Gong, G. Zhao, Q. G. Zhan, R. H. Zeng, Y. P. Cai, *Cryst. Growth Des.*, 2010, **10**, 4014-4022.
- 21 (a) M. W. Perkovic, *Inorg. Chem.*, 2000, **39**, 4962-4968; (b) Y. P. Huo, S. Z. Zhu, S. Hu, *Tetrahedron*, 2010, **66**, 8635-8640.
- 22 T. K. Kim, J. H. Lee, D. Moon, H. R. Moon, *Inorg. Chem.*, 2013, **52**, 589-595.